© creative

Scientific paper

Superparamagnetic Tragacanth Coated Fe₃O₄@SiO₂ Nanoparticles for the Loading and Delivery of Metformin

Fereshte Farajian¹ and Payman Hashemi^{1,*}

Department of Chemistry, Faculty of Science, Lorestan University, Khoramabad, I.R. Iran

* Corresponding author: E-mail: Hashemi.p@lu.ac.ir Phone: +986633120611

Received: 10-27-2021

Abstract

A novel superparamagnetic nano-composite of $Fe_3O_4@SiO_2$ coated by tragacanth gum (TG) as a natural product has been prepared. The obtained $SiO_2@Fe_3O_4@TG$ nanoparticles were characterized by Fourier transform infrared spectroscopy, energy dispersive X-ray analysis, scanning electron microscopy and dynamic light scattering analyzer. The magnetic nano-composite was applied for the loading and delivery of metformin, an oral diabetes medicine. The conditions for the loading of the drug were optimized by a central composite design optimization method. The maximum loading efficiency of the sorbent for metformin was obtained at pH 7 and its maximum *in-vitro* release was achieved at pH 1.6, using a phosphate-buffered saline medium. The loading capacity of the sorbent was dependent on the initial metformin concentration and exceeded to 19.6 mg/g in a 200 mg/L solution. A study of the adsorption isotherms for the drug indicated the best fitting into the Langmuir and Freundlich isotherms at the low and high metformin concentrations, respectively. The results indicated that the prepared $Fe_3O_4@SiO_2@TG$ adsorbent, as a non-toxic and low-cost sorbent, was quite appropriate for drug delivery applications.

Keywords: Tragacanth; Hydrogel adsorbent; Magnetic nanoparticles; Metformin

1. Introduction

In recent years, the interest forthe use of nanoparticles (NPs), especially magnetic NPs, for analytical purposes and in drug delivery applications has been increased. The major properties of magnetic NPs include easy separation by an external magnetic field, simple syntheses, high surface area, high firmness, reusability and biocompatibility.^{1,2} The superparamagnetic iron oxide core increases the binding capacity of NPs and enables them to replace the centrifugation step with magnetic separation. It also simplifies the application of NPs in immune assay.³ The oxidation potential of iron NPs is high and it is frequently necessary to coat their surfaces by mineral or organic compounds.⁴ SiO₂ is one of the materials used for coating ferrite NPs as it is non-toxic, water-dispersible, and environmentally friendly.5 Coating of magnetic NPs with biopolymers is also desirable as they can increase the adsorption capacity and selectivity of the NPs for numerous applications.6-9

Hydrogels are materials with swellable polymeric networks storing a great quantity of water. The potential to absorb water is due to the presence of polar and hydrophilic groups in the polymer network. The durability of hydrogels, on the other hand, is affected by crosslinking. Both artificial and natural polymers have been employed for the production of hydrogels. However, the natural polymeric hydrogels have several advantages such as high capacity of water absorption, low expense, long operation life, low toxicity, and high gel stability.¹⁰

Tragacanth gum (TG) is a natural adhesive mixture of polysaccharides obtained from the plant of *Astragalus* sp. It is a biosorbent and porous hydrogel material that is a non-toxic, abundant, low-cost and biocompatible biopolymer. Sp. 11 TG can be modified by various functional groups such as carboxylic acid, primary and secondary hydroxyl groups and epoxy groups which would enhance its selectivity and provide favourable adsorption conditions. The molecular structure of TG is shown in Figure 1. TG has been used in many applications such as wound covering, drug delivery, natural antibacterial and dispersing and thickening agent. TG is a biodegradable, biocompatible, inodorous, flavorless, osteogenic, and resistant biopolymer upon a wide pH range. However, the pure TG alone has some weaknesses and hence, it is

Figure 1. The chemical structure of TG.

frequently strengthened with either organic or inorganic materials such as clays,²⁰ carbon nanotubes²¹ methacrylate polymers,^{12,13} and metal nanoparticles.²²

The goal of the current study is to describe a novel synthesis of $Fe_3O_4@SiO_2@TG$ nanocomposite with an easy method as a magnetic adsorbent with biocompatibility, low toxicity, and low cost. The SiO_2 shell is anticipated to increase the resistance of the nanoparticles in acidic conditions and TG is a non-toxic drug delivery platform. The synthesized adsorbents would be studied for the loading and delivery of metformin as an oral diabetes medicine. In addition to the study of the adsorption mechanisms, multivariate methods are used for optimization of the loading conditions

2. Experimental Section

2. 1. Chemical and Apparatus

All applied chemicals were of analytical reagent grade and were used as received. Sodium hydroxide, ammonia solution 25%, tetraethyl orthosilicate (TEOS), ferric chloride (FeCl $_3$ 6H $_2$ O), ferrous chloride (FeCl $_2$ 4H $_2$ O) and ethanol were obtained from Merck chemical company.

A stock solution (1000 mg/g) of metformin was prepared by dissolving required quantity of the drug in methanol. Further dilutions were made by deionized water and prepared daily prior to use. Saline phosphate buffer solution (0.15 mol/L) was prepared by dissolving 0.8 g NaCl, 0.2 g KCl, 1.44 g Na₂HPO₄ and 0.24 g KHPO₄ in 1000 mL of distilled water. This solution was used for buffering test samples after adjustment of its pH (typically on 7.0). TG was obtained from local shops with the best quality and the pieces with transparent color were used for experiments. All solutions were prepared with deionized water.

All the spectrophotometric measurements of metformin were accomplished at its λ_{max} (232 nm) by a Shimadzu UV-1650PC UV-Vis spectrophotometer (Japan).

A pair of quartz cells (Esquartz, model Q124) were used for the measurements.

For the measurement of the hydrodynamic sizes and zeta potential values of $\text{Fe}_3\text{O}_4\text{@SiO}_2$ and $\text{Fe}_3\text{O}_4\text{@SiO}_2\text{@}$ GT particles as-prepared, a zeta potential and dynamic light scattering (DLS) analyzer, SZ-100 - HORIBA (Japan) was used. The particles were diluted with 20% ethanol in deionized water (pH 7).

2. 2. Synthesis of Fe₃O₄ NPs

For the preparation of ${\rm Fe_3O_4}$ NPs an ordinary chemical co-precipitation method was applied. ²³ In brief, 50 mL of 0.001 mol/L equimolar mixture of ${\rm FeCl_3}$ 6 H₂O, and ${\rm FeCl_2}$ 4 H₂O was prepared in deionized water. The mixture of the iron salts was sonicated for 15 min at room temperature. The mixture was then transferred to a round bottom two neck flask and heated to 80 °C under reflux in argon atmosphere. Then, 5 mL of concentrated ammonium hydroxide (25% w/w) was slowly added to it during 30 min. A color change from yellowish to black was observed in the mixture that was further heated to 90 °C for 1.5 h under the argon atmosphere. Next, the prepared ${\rm Fe_3O_4}$ nanoparticles were washed several times with deionized water after being separated by a permanent magnet.

Finally, the obtained ${\rm Fe_3O_4}$ NPs were re-suspended in 100 mL of deionized water. The obtained NPs were stable in this form up to two months.

2. 3. Synthesis of Fe₃O₄@SiO₂ NPs

Since hydrophobic Fe_3O_4 nanoparticles are unstable, they are usually coated by a silica shell.³ For silanization of the magnetic NPs a typical Stöber method was used. For this purpose, 1.5 g of Fe_3O_4 NPs were added to a solution of 16 mL distilled water, 80 mL ethanol and 2 mL 25% ammonia. The composition was then dispersed for 15 min in an ultrasonic bath. After that, 1.0 mL of tetraethyl

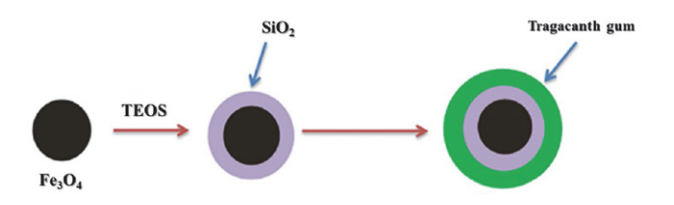


Figure 2. Schematic illustration of the procedure used for the synthesis of Fe_3O_4 @Si O_2 @GT NPs.

orthosilicate (TEOS) was added dropwise to the solution containing the NPs. The suspension was shaken on a shaker-bath for 24 h at room temperature. Eventually, the NPs were gathered by a permanent magnet and rinsed several times by distilled water.

2. 4. Coating of Fe₃O₄@SiO₂ NPs with TG

For the coating of the silanized magnetite NPs with TG, 0.02 g of TG powder was dissolved in 10 mL distilled water at 70 °C in a glass beaker. Subsequently, 1.5 g of $Fe_3O_4@SiO_2$ NPs were added to the solution under stirring at 1200 rpm and the solution was shaken for 4 h in room temperature. Finally, the $Fe_3O_4@SiO_2@TG$ NPs were washed by distilled water several times and the magnetic NPs were separated by a magnet (Figure 2) and stored in 20% ethanol.

2. 5. Central Composite Design (CCD) Optimization

A CCD method was used for the optimization of sample volume, adsorbent mass, pH and contact time. For each factor a low and high level was defined based on the results of some primary trials. For each of the four studied factors, five levels were suggested by the Minitab software as shown in Table 1.

The recovery or adsorption efficiency for the drug was regarded as the response or independent function for the optimization. The initiation of the design and statistical analyses of the results were performed using Minitab 16 software.

A drug concentration of 20 mg/L with the pH adjusted by a phosphate buffered saline solution (0.15 mol/L) was used during the optimization. After addition of the adsorbent, the mixture was shaken in a thermostated water

bath for a preset time and the ${\rm Fe_3O_4@SiO2@TG}$ particles were collected using a permanent magnet. The quantity of adsorbed metformin was computed by the absorbance measurements at 232 nm before and after the adsorption. Standard solutions of metformin in the range of 1 to 20 mg/L were utilized for the calibration.

2. 6 Calculation of the Adsorption Capacity

Adsorption capacity of the adsorbent was calculated in mg/g, by its loading with different metformin concentrations. This was done by adding 5 mg of the adsorbent to 1 mL of the drug solutions at pH 7. The residual amount of the drug in solution was calculated by absorption measurements at 232 nm using the UV/Vis spectrophotometer. The adsorption capacity was then calculated from equation 1:

$$q = [(C_o - C_t) \cdot V]/m \tag{1}$$

In this equation, q is the amount of analyte adsorbed or adsorption capacity (mg/g) of the adsorbent, C_o is the metformin concentration before addition of the sorbent and C_t represents its equilibrium concentration (mg/L), V represents the volume of the solution (L) and m is the adsorbent mass (g).

3. Results and Discussion

3. 1. Characterization of the NPs

In the introductory experiments, Fe₃O₄, Fe₃O₄@SiO₂ and Fe₃O₄@SiO₂@TG magnetic NPs were prepared and characterized by Fourier transform infrared spectroscopy (FT-IR), energy dispersive X-ray analysis (EDX), scanning electron microscopy (SEM) and dynamic light scattering (DLS) analyzer. Figure 3 shows the FT-IR spectra of the NPs. In the FT-IR spectrum of Fe₃O₄ NPs (Figure 3a), the peak that appeared at wavenumber 584 cm⁻¹ is related to stretching vibrations of Fe-O. The bands in the range of 1200-1000 cm⁻¹ in (Figure 3b and 3c) belong to the Si-O covalent bond vibrations and confirms the coating of silica on nanoparticles. In the FT-IR spectra associated with Fe₃O₄@SiO₂@TG magnetic NPs (Figure 3c), other major vibrational peak in 3712 cm⁻¹ is related to stretching vibration of C-H. This band is a proof of the fixation of TG layer on Fe₃O₄@SiO₂ magnetic NPs.

Table 1. The studied parameters and suggested levels in the CCD optimization.

Factor	Abbreviation	Factors' levels					
		-α	Low	0	High	+α	
pН	рН	2	3.5	5	6.5	8	
Contact time (min)	Time	20	30	40	50	60	
Temperature (°C)	T	25	30	35	40	45	
Sample volume (mL)	V_s	1	3	5	7	9	

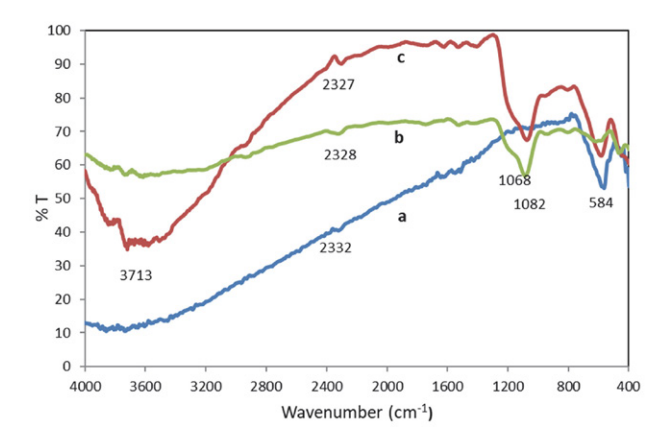


Figure 3. FT-IR spectra of Fe_3O_4 (a), Fe_3O_4 @ SiO_2 (b) and Fe_3O_4 @ SiO_2 @TG (c) nanoparticles.

The dimension and morphology of Fe $_3O_4$, Fe $_3O_4$ @ SiO $_2$ and Fe $_3O_4$ @SiO $_2$ @TG nanoparticles were evaluated by SEM. Figure 4 shows the spherical morphology and narrow size spreading of the NPs with an average size of 50–70 nm for Fe $_3O_4$ @SiO $_2$ @TG. Energy dispersive X-ray (EDX) analysis was used for the elemental mappings and distribution of the prepared Fe $_3O_4$ @SiO $_2$ and Fe $_3O_4$ @SiO $_2$ @TG nanoparticles. Based on the EDX results, C, N, O, Si and Fe were recognized in the study of Fe $_3O_4$ @SiO $_2$ @TG nanoparticles and as expected, the quantity of carbon in the Fe $_3O_4$ @SiO $_2$ @TG nanoparticles was more than that of Fe $_3O_4$ @SiO $_2$ due to the presence of TG in the former. The results apparently confirm covering of the nanoparticles by TG.

Zeta potential study of $Fe_3O_4@SiO_2$ and GT coated adsorbents indicated a -26.6 mV potential for the $Fe_3O_4@SiO_2$ and -23 mV for the $Fe_3O_4@SiO_2@GT$ adsorbent. This indicates that coating of the adsorbent with GT only slightly reduces the negative charge of it. The DLS results indicated that the hydrodynamic sizes of the adsorbents

are increased to 191 and 253 nm, respectively. It also showed some swelling of the SiO_2 and TG shells in solution that confirms a biocompatible coating for the incorporation of the drug.²⁴

3. 2. Effect of pH on Adsorption

One of the important parameters in analyzing adsorption systems is pH, that influences both the chemistry of the sample and the adsorbent binding sites. ²⁵ In the present study, the efficacy of pH on the adsorption or loading the drug was investigated in a range of pH = 2-11 with an primary drug concentration of 20 mg/L and using 50 mg of the adsorbent in a mixing time of 30 min (Figure 5). As shown in the figure, by increasing pH from 2 to 7, the adsorption efficiency increases, so that at pH 7, the highest loading is obtained. At higher pH values, a moderate decrease in the efficiency is observed. Alteration of pH can change the surface charge of magnetic NPs. ²⁶ More negative surface charges are expected at a higher pH that is more suitable for the extraction of metformin. This

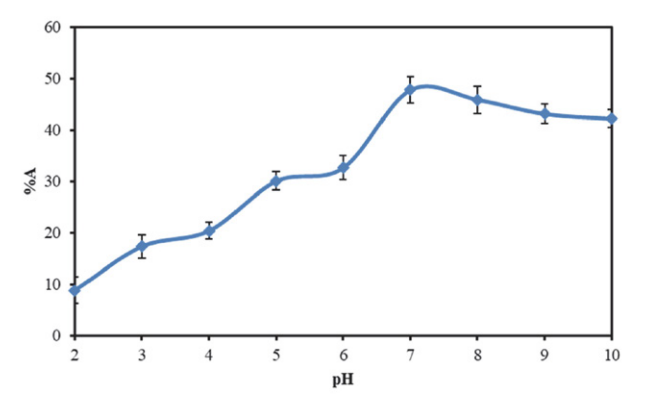
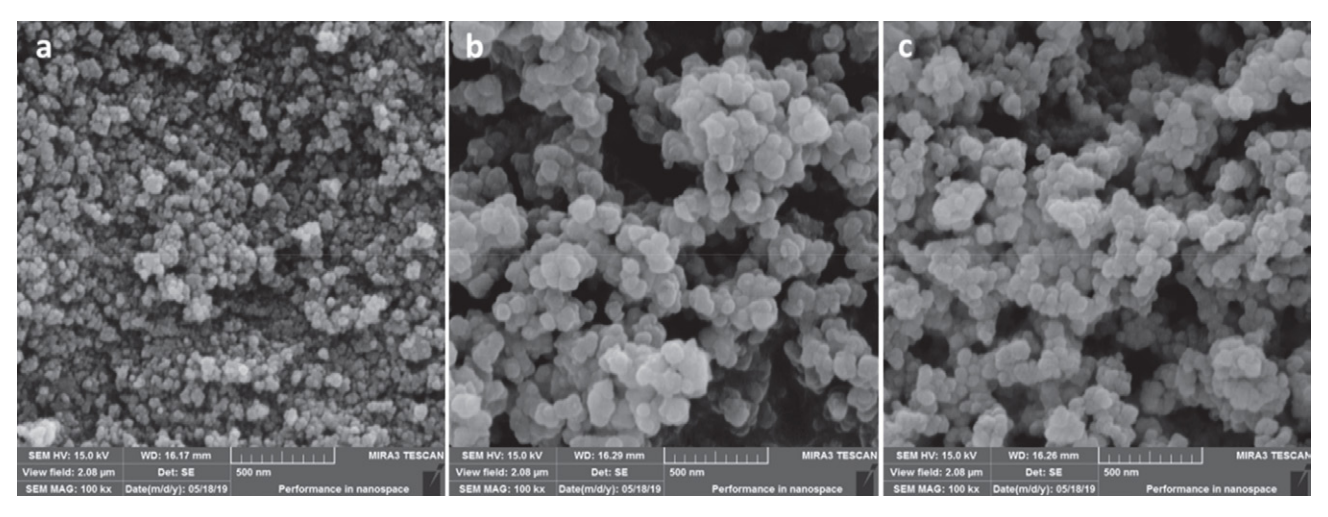


Figure 5. Effect of pH on the adsorption of metformin on the Fe_3O_4 @SiO_2@TG NPs. Sample volume, 5 mL; adsorbent mass, 50 mg; drug concentration, 20 mg/L; mixing time, 30 min; temperature, 25 °C.



 $\textbf{Figure 4.} \ \text{SEM images of Fe}_3O_4(a), \ \text{Fe}_3O_4@SiO_2(b) \ \text{and Fe}_3O_4@SiO_2@GT \ (c) \ MNPs.$

is supported by the increase in the adsorption efficiency up to pH 7 in Figure 5.

3. 3. Optimization of the Adsorption Conditions

A central composite design (CCD) method was used for the optimization of the loading of metformin on the adsorbent. CCD is one of the most usual multifunctional optimization techniques. In this process, two low and high levels are defined for each factor with the addition of at least one center point and some axial or star points. With this pattern, the approximation of both linear and quadratic effects are possible.²⁷ For a reasonable estimation of the experimental error, replicate analyses are performed on the center points.²⁸

Four factors of pH, temperature (T), volume of sample (Vs) and contact time (Time) were studied and optimized by the CCD model. The five levels designed for

Table 2. Conditions of the performed tests and their related adsorption efficiency attained by the experiments in the CCD optimization.

Run order	pН	V _s (mL)	Time (min)	T (°C)	Adsorption (%)
1	10	3	50	30	45.8
2	8	<i>3</i> 7	50 50	30	
3	8 9	9	40	35	44.9
4	9	5	40	35 35	31.7 44.6
5	9	5	40	35 35	55.1
6	9	5 5	60	35 35	
					44.5
7 8	8 8	3	30 50	30 30	75.6
					68.9
9	8 9	3	30	40	60.0
10		5	40	25	44.1
11	9	5	40	35	44.9
12	10	3	50	40	61.4
13	11	5	40	35	57.3
14	8	7	30	30	47.9
15	10	3	30	30	63.8
16	10	3	30	40	63.8
17	9	1	40	35	79.0
18	10	7	30	40	36.4
19	10	7	30	30	41.8
20	9	5	40	35	51.5
21	9	5	40	35	59.2
22	9	5	40	35	48.3
23	9	5	40	35	56.6
24	8	7	30	40	36.0
25	8	7	50	40	38.0
26	7	5	40	35	31.7
27	10	7	50	40	61.3
28	8	3	50	40	67.0
29	9	5	40	45	58.9
30	10	7	50	30	44.7
31	9	5	20	35	44.6

each factor is shown in Table 1. The levels of the factors in 31 planned experiments by the model and the received response values for each experiment is shown in Table 2. Optimization of the studied factors were accomplished using a response surface model. Some three-dimensional response plots are shown in Figure 6 to demonstrate how the response variable changes with variation of a pair of factors while all other factors stay constant.

As shown in Figure 6a, at a high pH, an increase in adsorption is observed with time, while at a lower pH, such effect is not considerable which indicates the rapid adsorption of metformin on the adsorbent. Figure 6b demonstrates the interaction between pH and temperature (T); at a low temperature, adsorption is decreased by increasing the pH but at a higher temperature, it is slightly increased. In Figure 6c it is shown that at a low sample volume, adsorption efficiency is increased by time, while an opposite effect is observed at a higher sample volume. The same or even more remarkable effect is detected for the dual effect of pH and sample volume (not shown in the figure).

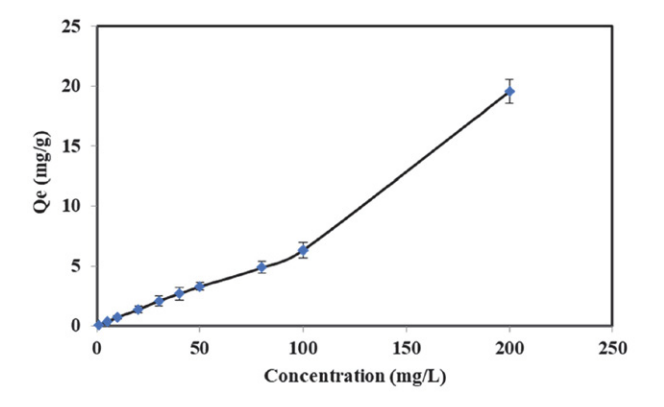


Figure 6. Three-dimensional surface plots in CCD optimization procedure. (a) Effects of pH and contact time, (b) Effects of pH and temperature (T), (c) Effects of contact time and volume of sample (V_s).

Table 3 displays the results of the data analysis by the CCD model for the discrete and combined effects and second order interactions of the studied variables. Based on the t-test results, the most considerable variable is the sample volume with a large negative effect on the adsorption efficiency. The other factors are statistically negligible with the order of pH > T > Time. The squared terms of the factors are also negligible but the pH \times T and Time \times T interactions may be considered notable at a 90% confidence level.

The anticipated optimized conditions suggested by the model for the whole data were as follows: pH = 7, temperature = 25 °C, volume of sample = 1.0 mL, and contact time = 20 min. By execution of 6 replicated analyses in the optimum conditions, an adsorption efficiency of 83.27(\pm 6.45) % was obtained for metformin.

Table 3. Effects of the factors, coded coefficients (Coef), standard errors (SE) of the coefficients, t-values and p-values of the variables obtained by the CCD model.

Term	Effect	Coef	SE Coef	T-Value	P-Value
Constant		51.46	2.89	17.81	0.000
pН	2.66	1.33	1.56	0.85	0.407
Time	0.54	0.27	1.56	0.17	0.864
T	1.68	0.84	1.56	0.54	0.599
Vs	-20.82	-10.41	1.56	-6.67	0.000
рН×рН	-1.94	-0.97	1.43	-0.68	0.507
Time×Time	-1.92	-0.96	1.43	-0.67	0.512
$T \times T$	1.56	0.78	1.43	0.54	0.594
Vs×Vs	3.48	1.74	1.43	1.22	0.241
pH×Time	1.01	0.51	1.91	0.26	0.795
рН×Т	7.89	3.94	1.91	2.06	0.056
pH×Vs	6.76	3.38	1.91	1.77	0.096
Time×T	7.04	3.52	1.91	1.84	0.084
Time×Vs	5.86	2.93	1.91	1.53	0.145
$T \times Vs$	-0.71	-0.36	1.91	-0.19	0.854

3. 4. Adsorption Capacity

The adsorption capacity of the $\rm Fe_3O_4@SiO_2@TG$ adsorbent or its maximum metformin loading was associated with the primary concentration of the drug in the sample. The capacity was calculated by suspending variant amounts of the adsorbent in a buffered solution of the analyte, under the optimum conditions. The effect of primary concentration of metformin on the adsorption capacity is shown in Figure 7. The adsorption capacity of the nanocomposite increased with increasing the primary concentration of metformin. The maximum capacity obtained for 200 mg/L of metformin was 19.6 mg/g.

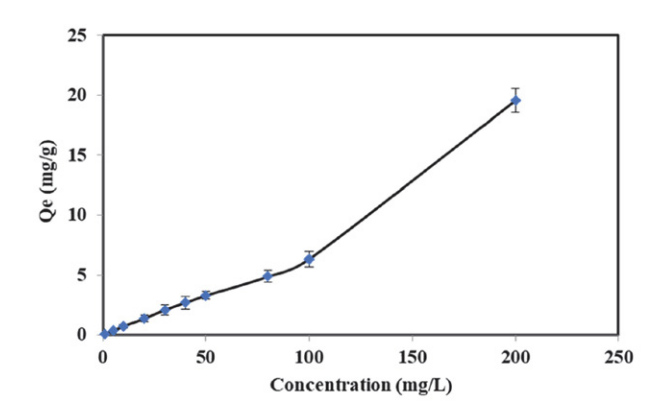
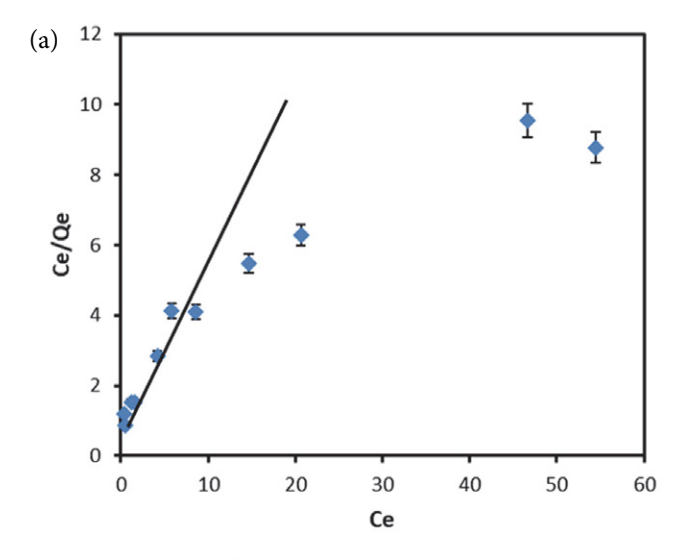


Figure 7. The adsorption capacity of NPs as a function of the initial concentration of metformin under the optimized conditions; pH, 7; T, 25 °C; t, 20 min; sample volume, 1.0 mL; adsorbent mass, 40 mg; number of replicates, 3.

3. 5. Study of the Adsorption Isotherms

The mechanism of interaction of metformin with the adsorbent was examined by studying the adsorption isotherms in batch experiments. For the analysis of the experimental data, two adsorption models of Langmuir and Freundlich were used. The Langmuir adsorption isotherm relates the monolayer adsorption of a species onto the adsorbent superficial with some well-defined sites. According to this model, the plot of C_e/q , in which C_e is the equilibrium concentration of the analyte in solution and q is the balanced adsorption capacity of the sorbent, versus C_e should be linear. The Freundlich isotherm is not restricted to the formation of a monolayer and is related to the reversible adsorption. Accordingly, a linear plot is attained for plotting $\log q$ versus $\log C_e$.

Figure 8a and 8b are the corresponding plots of the Langmuir and Freundlich models, respectively. Regarding R^2 as an indication of the desirable fit of experimental data, the Langmuir adsorption is more appropriate at lower than 5.8 mg/L C_e values suggesting the monolayer adsorption of metformin at low metformin concentrations. At higher C_e values, however, the Freundlich adsorption,



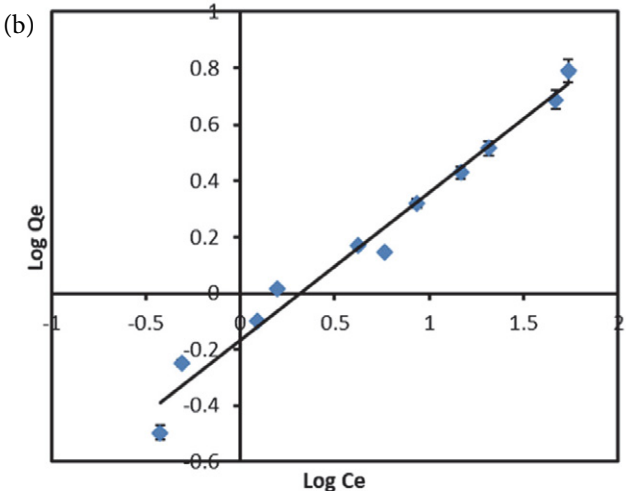


Figure 8. a The Langmuir adsorption isotherm and ${\bf b}$ The Freundlich adsorption isotherm for the results shown in Figure 7.

with an R^2 value of 0.9772, is more appropriate than the Langmuir adsorption indicating the possibility of multi-layer adsorption mechanism in this region. The values of b (Langmuir constant), $q_{\rm m}$ (maximum one-layer adsorption capacity), $k_{\rm F}$ and n (Freundlich constants) were computed to be 1.36 L/mg, 1.81 mg/g, 0.68, and 1.91, respectively. The Freundlich constant n is higher than one, representing the appropriate conditions for the adsorption. n

3. 6. Evaluation of Drug Release

The influence of contact time on the desorption or the release rate of metformin from the prepared adsorbent was studied in a range from 5 to 50 min. Metformin was first loaded on the adsorbent at the optimized conditions (pH 7, volume of sample 1.0 mL, T 25 C, and contact time 20 min). The desorption was accomplished using phosphate buffered saline at three different pH values of 1.6, 3.0, and 7.3. The low pH values were selected as the region with minimum adsorption of metformin (see Figure 5). The release at pH 7.3 was also studied because this is the pH of the human body.

The corresponding results are shown in Figure 9. The maximum drug desorption or delivery was obtained within 10 to 30 min by changing the pH from 1.6 to 3.0 and a maximum delivery of 85% was obtained at pH 3.0. It is also seen that at the body pH of 7.3 some 38% delivery is observed which may be useful when the drug is used for intravenous injections.

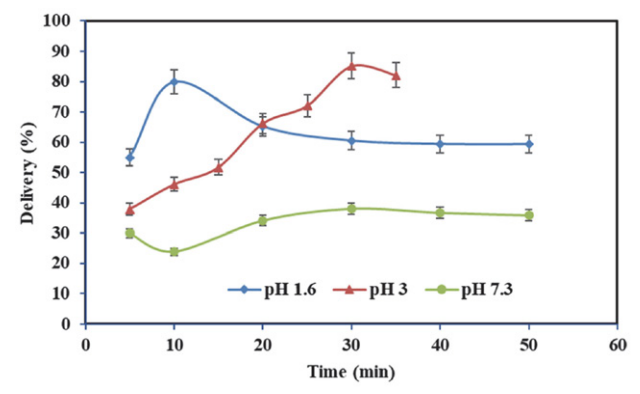


Figure 9. Metformin desorption (delivery) from the loaded $Fe_3O_4@$ $SiO_2@TG$ NPs in pH 1.6, 3.0 and 7.3. Number of replicates: 3.

4. Conclusions

Coating of $Fe_3O_4@SiO_2$ magnetic NPs by TG as a natural hydrogel was successfully carried out using a simple modifying process. Characterization of the prepared NPs by FT-IR, EDX and SEM corroborated the structure and the relatively uniform sizes of the prepared NPs. The results demonstrated that the synthesized $Fe_3O_4@SiO_2@TG$ nanocomposite is a suitable carrier for the loading and

releasing of metformin, as it is non-toxic, highly porous, low cost, and biocompatible.

The modified nanocomposite established a high efficiency for metformin adsorption with a loading capacity up to 19.6 mg/g in a short time. The adsorption on the prepared NPs fitted into Langmuir isotherm at low concentrations of metformin while it was best fitted into Freundlich isotherm in a higher concentration area. Maximum desorption of the medicine happened in pH of 1.6 to 3.0 within 10 to 30 min. The results indicated the potential use of the Fe $_3$ O $_4$ @ SiO $_2$ @TG adsorbent as an inorganic-organic hybrid for the loading and delivery of metformin and possibly for the removal of pharmaceutical residues in the environment.

5. References

1. A. A. Alqadami, M. Naushad, M. A. Abdalla, T. Ahamad, Z. A. ALOthman, S. M. Alshehri, A. A. Ghfar, *Journal of Cleaner Production* **2017**, *156*, 426–436.

DOI:10.1016/j.jclepro.2017.04.085

- A. A. Alqadami, M. Naushad, M. A. Abdalla, M. R. Khan, Z. A. Alothman, *Journal of Chemical & Engineering Data* 2016, 61, 3806–3813. DOI:10.1021/acs.jced.6b00446
- 3. K. Hemmati, A. Masoumi, M. Ghaemy, *Carbohydrate polymers* **2016**, *136*, 630–640. **DOI**:10.1016/j.carbpol.2015.09.006
- 4. C. Singh, A. Goyal, S. Bansal, S. Singhal, *Materials Research Bulletin* **2017**, 85, 109–120.

DOI:10.1016/j.materresbull.2016.09.010

- 5. M. Coşkun, M. Korkmaz, Journal of nanoparticle research **2014**, *16*, 2316. **DOI:**10.1007/s11051-014-2316-3
- S. Hanif, A. Shahzad, Journal of nanoparticle research 2014, 16, 2429. DOI:10.1007/s11051-014-2429-8
- 7. A. Mittal, R. Ahmad, I. Hasan, Desalination and Water Treatment 2016, 57, 19820–19833.

DOI:10.1080/19443994.2015.1104726

- S. Nasirimoghaddam, S. Zeinali, S. Sabbaghi, Journal of Industrial and Engineering Chemistry 2015, 27, 79–87.
 DOI:10.1016/j.jiec.2014.12.020
- 9. S. Sadeghi, F. A. Rad, A. Z. Moghaddam, *Materials Science* and Engineering: C **2014**, 45, 136–145.

DOI:10.1016/j.msec.2014.08.063

- E. M. Ahmed, *Journal of advanced research* **2015**, *6*, 105–121.
 DOI:10.1016/j.jare.2013.07.006
- R. Sahraei, Z. S. Pour, M. Ghaemy, Journal of cleaner production 2017, 142, 2973–2984. DOI:10.1016/j.jclepro.2016.10.170
- K. Hemmati, A. Masoumi, M. Ghaemy, *Polymer* **2015**, *59*, 49–56. **DOI:**10.1016/j.polymer.2014.12.050
- 13. K. Hemmati, A. Masoumi, M. Ghaemy, *RSC advances* **2015**, *5*, 85310–85318. **DOI:**10.1039/C5RA14356J
- 14. B. Singh, L. Varshney, S. Francis, *Radiation Physics and Chemistry* **2017**, *135*, 94–105.

DOI:10.1016/j.radphyschem.2017.01.044

B. Singh, V. Sharma, *Carbohydrate polymers* **2017**, *157*, 185–195. **DOI:**10.1016/j.carbpol.2016.09.086

- 16. M. Nasiri, M. Barzegar, M. A. Sahari, M. Niakousari, *Food Hydrocolloids* **2017**, *72*, 202–209.
 - **DOI:**10.1016/j.foodhyd.2017.05.045
- 17. A. Komeilyfard, M. Fazel, H. Akhavan, A. Mousakhani Ganjeh, *Journal of texture studies* **2017**, *48*, 114–123.
 - **DOI:**10.1111/jtxs.12216
- R. Sahraei, M. Ghaemy, Carbohydrate polymers 2017, 157, 823–833. DOI:10.1016/j.carbpol.2016.10.059
- S. Kulanthaivel, S. R. VS, T. Agarwal, S. Pradhan, K. Pal, S. Giri, T. K. Maiti, I. Banerjee, *Journal of Materials Chemistry B* 2017, 5, 4177–4189. DOI:10.1039/C7TB00390K
- S. Pirsa, F. Mohtarami, S. Kalantari, Chemical Review and Letters 2020, 3, 98–103.
- S. Mallakpour, F. Tabesh, International Journal of Biological Macromolecules 2021, 166, 722–729.
 - DOI:10.1016/j.ijbiomac.2020.10.229
- A. Bahrami, R. R. Mokarram, M. S. Khiabani, B. Ghanbarzadeh, R. Salehi, *International journal of biological macromole*cules 2019, 129, 1103–1112.
 - DOI:10.1016/j.ijbiomac.2018.09.045

- 23. M. Faraji, Y. Yamini, E. Tahmasebi, A. Saleh, F. Nourmohammadian, *Journal of the Iranian Chemical Society* **2010**, *7*, S130–S144. **DOI**:10.1007/BF03246192
- 24. J. Szűcsová, A. Zeleňáková, O. Kapusta, A. Berkutova, V. Zeleňák, in Book Influence of silica coating on magnetic properties and Zeta potential of Fe3O4@ mSiO2 core-shell for drug delivery systems, ed., ed. by Editor, AIP Publishing LLC, City, 2018, Vol. 1996, Chap. Chapter, pp. 020047.
 DOI:10.1063/1.5048899
- Z. L. Yaneva, N. V. Georgieva, International Review of Chemical Engineering 2012, 4, 127–146.
- K. Ahalya, N. Suriyanarayanan, S. Sangeetha, *Materials science in semiconductor processing* 2014, 27, 672–681.
 DOI:10.1016/j.mssp.2014.08.009
- M. A. Bezerra, R. E. Santelli, E. P. Oliveira, L. S. Villar, L. A. Escaleira, *Talanta* 2008, *76*, 965–977.
 DOI:10.1016/j.talanta.2008.05.019
- 28. F. N. Serenjeh, P. Hashemi, M. Safdarian, Z. Kheirollahi, *Journal of the Iranian Chemical Society* **2014**, *11*, 733–739. **DOI:**10.1007/s13738-013-0346-x
- F. G. Adivi, P. Hashemi, A. D. Tehrani, *Polymer Bulletin* 2019, 76, 1239–1256. DOI:10.1007/s00289-018-2418-7

Povzetek

Pripravili smo nov superparamagnetni nanokompozitni material iz Fe₃O₄@SiO₂, prevlečen s tragakantovim gumijem (TG) kot naravnim proizvodom. Pridobljene SiO₂@Fe₃O₄@TG nanodelce smo okarakterizirali z infrardečo spektroskopijo s Fourierjevo transformacijo, energijsko-disperzno rentgensko žarkovno analizo, vrstično elektronsko mikroskopijo in dinamično analizo svetlobnega sipanja. Magnetni nanokompozitni material smo uporabili za vezavo in sproščanje metformina, oralne učinkovine proti diabetesu. Pogoje za vezavo učinkovine smo optimizirali s pomočjo metode faktorskega načrta. Največjo vezavno učinkovitost sorbenta za metformin smo dobili pri pH 7, maksimalno *in-vitro* sproščanje v salinem mediju s fosfatnim pufrom pa pri pH 1,6. Vezavna kapaciteta sorbenta je bila odvisna od začetne koncentracije metformina in je dosegla 19,6 mg/g v raztopini s koncentracijo 200 mg/L. Študij adsorpcijskih izoterm za učinkovino je pokazal najboljše prileganje Langmuirjevi izotermi pri nizkih koncentracijah in Freundlichovi izotermi pri visokih koncentracijah metformina. Rezultati dokazujejo, da je pridobljeni Fe₃O₄@SiO₂@TG adsorbent, ki je nestrupen in cenen, povsem primeren za uporabo pri dostavi zdravilnih učinkovin.



Except when otherwise noted, articles in this journal are published under the terms and conditions of the Creative Commons Attribution 4.0 International License